

The crystallization behaviour of bismuth germanate glasses

L. DIMESSO, G. GNAPPI, A. MONTENERO

Istituto di Strutturistica Chimica, Università degli Studi di Parma, Viale delle Scienze, 43100 Parma, Italy

P. FABENI, G. P. PAZZI

I.R.O.E. C.N.R., Via Panciatichi 64, 50127 Firenze, Italy

Glassy samples containing Bi_2O_3 and GeO_2 in different ratios were prepared and absorption measurements were performed on the samples in the ultraviolet region in order to determine the optical behaviour. Thermal analysis performed on the vitreous samples gave the glass transition temperature and the crystallization temperature. The main crystalline phases separated during the heat treatment were $\text{Bi}_4\text{Ge}_3\text{O}_{12}$ (BGO) and Bi_2GeO_5 . The activation energy of the crystallization process of the sample BGO (1:3) was measured using the isothermal method, and the value obtained was $47.1 \text{ kcal mol}^{-1}$; the reaction order was equal to 1.1.

1. Introduction

Bismuth germanate $\text{Bi}_4\text{Ge}_3\text{O}_{12}$ (BGO) is a synthetic crystal having the same structure of mineral $\text{Bi}_4\text{Si}_3\text{O}_{12}$ (eulytite). These crystals have been studied since the 1950s for their electro-optical [1, 2], electromechanical [3] and luminescence properties [4]. In the 1980s, BGO received much attention because of its physical properties which make it suitable to replace traditional scintillators such as NaI(Tl) and CsI(Na) .

Among the applications of BGO, the most important are in nuclear medicine (X-ray and positron emission tomography), in fundamental research (telescopes for hard-X and γ -rays in astrophysics and nuclear physics) and in industry (well logging, control of fusion processes). In particular, BGO is very useful for the construction of compact high-resolution electromagnetic calorimeters for high-energy physics [5].

To produce these crystals successfully, a detailed fundamental knowledge of the growth behaviour is necessary. Moreover, the growth of BGO monocrystals presents some difficulties [6–9] due to its physical features. Only high-purity oxides give high-quality BGO monocrystals and the two oxide powders must be mixed very accurately to avoid deviation from the stoichiometric composition.

Another aspect to be taken into account is the precise temperature control, because the driving force of the crystal growth from the melt is supercooling, so any fluctuation at the solid–liquid interface may produce defects in the crystal structure. Such defects, comprising non-stoichiometric phases, bubbles and insoluble foreign particles, will reduce considerably the crystal performances (e.g. energy resolution).

The aim of this work was to study the thermal behaviour of the Bi_2O_3 – GeO_2 glassy system in order to obtain polycrystalline specimens and to make a

comparison between the properties of the monocrystal and the polycrystalline material.

There are some advantages in obtaining BGO polycrystalline samples via the glassy route. In fact, it is easier to prepare glassy samples than a crystal, and furthermore, in the devitrification process, a precise control of the temperature is not as important as in crystal growth. The phase diagram of bismuth and germanium oxides, presented in Fig. 1 [5], shows the possibility of obtaining four different crystalline compounds as a function of their well-defined proportions. Therefore, we prepared and studied the same compositions (indicated by dots in the figure) as glassy samples.

2. Experimental procedure

The samples were obtained by melting in an electric furnace under air atmosphere. The melting temperature, chosen as a function of the composition [10], was in the range 1473–1573 K and the batch powders were introduced into the previously heated furnace in order to avoid oxide losses caused by the surface tension, especially for Bi_2O_3 . The melts were quenched using a melt-spinning apparatus, because the ultra-high cooling rate (about 10^6 K min^{-1}) was able to give glassy samples (flakes) and to avoid any phase separation.

These flakes were analysed using a Philips inductively coupled plasma (ICP) spectrometer Model PU7450. Samples were dissolved in diluted HCl to avoid the formation of insoluble hydroxides. The composition of the samples is reported in Table I.

The samples are identified by the symbol BGO($x:y$), ($x:y$) being the molar ratio $\text{Bi}_2\text{O}_3:\text{GeO}_2$. They were prepared from extra-pure powdered oxides

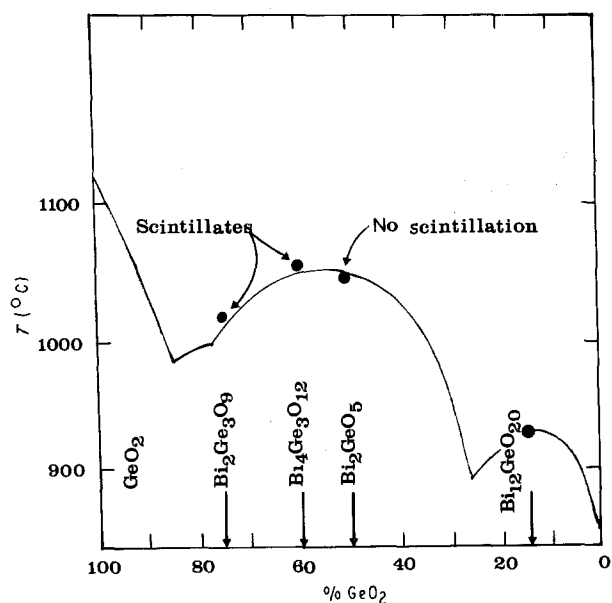


Figure 1 Phase diagram of $\text{Bi}_2\text{O}_3\text{-GeO}_2$ [5].

TABLE I Theoretical and experimental composition of BGO samples (% wt/wt)

BGO	Theoretical		Experimental	
	Bi	Ge	Bi	Ge
1:3	53.6	28.0	53.1	27.3
2:3	67.1	17.4	64.3	17.2
1:1	73.1	12.7	72.8	12.3
6:1	86.5	2.5	84.0	2.4

(Bi_2O_3 Fluka, GeO_2 Ventron-Alfa Produkte). Ultraviolet spectra were recorded using a Kontron spectrophotometer Model Uvikon 860.

The presence of crystalline phases, obtained after heat treatment, was investigated by powder X-ray diffraction (XRD, Philips PW 1710 Diffractometer, CuK_α radiation). These phases have been identified by comparing the XRD patterns with those reported in the literature [11].

Thermal analyses were performed using a Perkin Elmer differential scanning calorimeter DSC-7 Delta instrument.

3. Results and discussion

3.1. Ultraviolet absorption measurements

To date there has been no systematic study of the optical properties of these glasses in the ultraviolet region. Experimental investigations of the dependence of these properties on the glassy network, temperature and composition, and theoretical analyses of the mechanism of ultraviolet absorption in vitreous materials have just begun [12].

The absorption processes in the ultraviolet region involve, basically, two types of electronic transition. The first is the promotion of an electron from a localized orbital on one ion, either to a higher but still localized orbital or to a collective energy level for the

system – “the conduction band”. In this case, if the excited electron is localized on the same ion or molecule, the new state is described as an “exciton” and the associated absorption band is called an exciton band. However, if the excitation transfers the electron to an orbital lying completely or partly on another atomic species, then the observed absorption is generally called a “charge transfer” process, which is the second case.

The shape of the spectra is different for the two mechanisms: in the case of excitation into a conduction band, the absorption coefficient rises with decreasing photon wavelength to a plateau value, while a transition to a non-localized orbital would result in a normal optical band with a well-defined maximum value.

Stevels [13] pointed out that for the most conventional oxides glasses, which contain only light electro-positive cations, the conduction band lies at very high energies and ultraviolet absorption is due to transitions of the exciton type. In a glass containing heavier cations (e.g. Cd(II) germanate glasses [12]), the conduction band lies at lower energies and may overlap the exciton levels, with the result that such glasses have an absorption edge near the visible and are photoconducting.

Fig. 2 shows the BGO(2:3) ultraviolet spectrum: because of instrumental limits, it is impossible to reveal the shape of the spectrum for values of absorbance over 4.0 because the absorption is too strong. Reisfeld and Boehm [14] overcame the problem by comparing absorption and excitation spectra of Bi^{3+} in phosphate, borax and germanate glasses. From this comparison they could derive for a bismuth-germanate glass an absorption peak whose maximum is at about 270 nm. So, we can suppose a charge-transfer process for ultraviolet absorption in BGO glasses.

The absorption coefficients for most processes occurring in the ultraviolet field are of the order of $10^4\text{-}10^6\text{ cm}^{-1}$ [12]. Consequently, very thin samples are required if complete absorption bands are to be recorded. Such samples are not easy to prepare and in any case they are not representative of the bulk material.

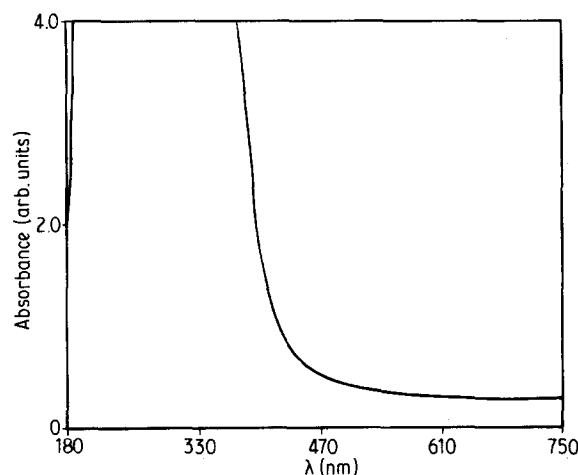


Figure 2 Ultraviolet spectrum of sample BGO(2:3).

Most of the ultraviolet absorption studies on glassy systems have thus been limited to measurements of an absorption edge, defined as the short wavelength transmittance limit of cut-off wavelength, λ_0 . λ_0 is not a well-defined parameter and has been taken as the wavelength where the transmittance in a given sample thickness can just be measured, usually 0.5% [12]. In Fig. 3 cut-off wavelengths as a function of the molar ratio $\text{Bi}_2\text{O}_3/\text{GeO}_2$ are shown; all the samples had the same thickness ($65 \pm 3 \mu\text{m}$). It is possible to see that the value of λ_0 decreases as the GeO_2 content in the glasses increases, and therefore the gap between the energy levels is increased. This is in agreement with the low values of λ_0 reported for vitreous GeO_2 (325–220 nm) [12].

3.2. DSC and XRD analyses

ICP analyses revealed that although a possible slight loss of bismuth oxide during the melting process was noted, the effective composition of the samples does not differ from the theoretical one, as shown in Table I.

The glasses were subjected to thermal analysis in order to investigate their thermal behaviour, as well as to analyse the crystallization kinetics.

All DSC thermograms were measured up to 998 K with a 20 K min^{-1} heating rate. From these data the crystallization temperature, T_c , was determined (reported in Table II); T_c was chosen as the maximum temperature for performing heating cycles on all the samples. All these heating schedules were performed with a dwell time of 6 h at the temperature T_c .

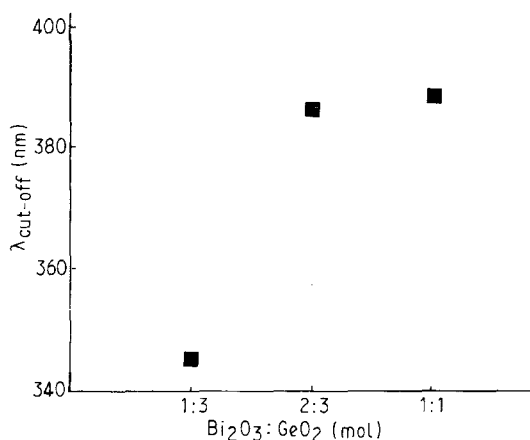
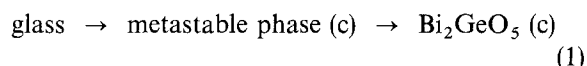


Figure 3 Cut-off λ_0 as a function of the molar ratio $\text{Bi}_2\text{O}_3/\text{GeO}_2$. Errors are smaller than the point size.

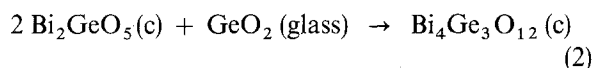
TABLE II Crystalline phases formed after heat treatment

BGO	T_c ($\pm 0.1 \text{ K}$)	Dwell (h)	Crystalline phases
1:3	840	6	$\text{Bi}_4\text{Ge}_3\text{O}_{12}$
2:3	868	6	Bi_2GeO_5 , $\text{Bi}_4\text{Ge}_3\text{O}_{12}$
	916	6	$\text{Bi}_4\text{Ge}_3\text{O}_{12}$, Bi_2GeO_5
1:1	758	6	Bi_2GeO_5
6:1	752	6	$\text{Bi}_{12}\text{GeO}_{20}$

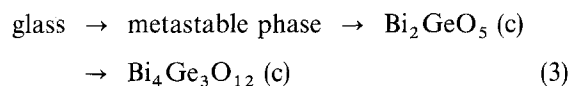
In the DSC thermogram of BGO(1:1), shown in Fig. 4, it is possible to note the presence of two peaks, the greatest corresponding to Bi_2GeO_5 crystallization. To confirm Bi_2GeO_5 as a separated crystalline phase, the experimental XRD spectrum, not reported in literature [11], was compared with the calculated one by means of the LAZY PULVERIX program [15]. The smallest peak, at 733 K (onset = 723 K), might be a thermal signal due to a metastable phase with structure very similar to that of Bi_2GeO_5 [16]. This would suggest that the following solid–solid reaction inside glassy BGO(1:1) takes place (c is the crystalline phase)



Thermal treatments of sample BGO(2:3), at 868 and 916 K, respectively, yielded Bi_2GeO_5 with a small amount of $\text{Bi}_4\text{Ge}_3\text{O}_{12}$ phase at lower temperature and $\text{Bi}_4\text{Ge}_3\text{O}_{12}$ with a small amount of Bi_2GeO_5 at higher temperature. It was impossible to obtain these phases separately. Reaction 1 can explain this behaviour. In fact, because of the greater amount of GeO_2 in the sample, the Bi_2GeO_5 formed would react almost completely, according to the following reaction



As stated previously, the major separated crystalline phase at lower T_c is Bi_2GeO_5 ; this means that it is kinetically favoured over the formation of $\text{Bi}_4\text{Ge}_3\text{O}_{12}$, while the latter is thermodynamically more stable. Then the overall solid–solid reaction can be written



Reaction 3 confirms that Bi_2GeO_5 itself is a metastable phase in the crystallization process. Many researchers [6, 17] have confirmed the presence of metastable Bi_2GeO_5 , obtained after quick cooling of melts with BGO(2:3) stoichiometry.

For the BGO (6:1) sample, the DSC thermogram shows only one peak at 752 K, due to the separation of the crystalline phase with stoichiometry corresponding to the starting composition $\text{Bi}_{12}\text{GeO}_{20}$, as confirmed by XRD analysis. However, after 6 h thermal

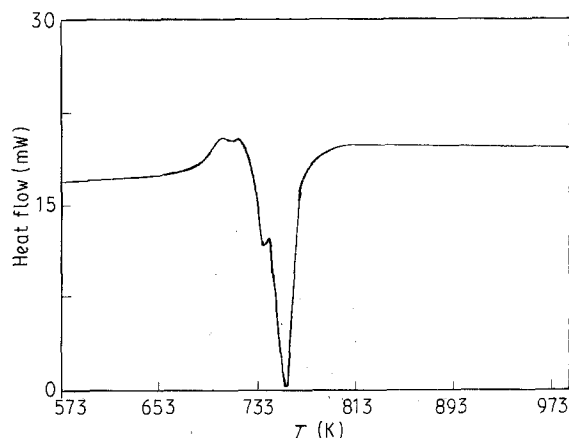
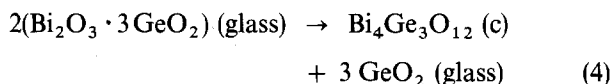


Figure 4 DSC thermogram of sample BGO(1:1).

treatment at the peak temperature, the presence of a large amount of the glassy phase was still noted, indicating a very slow kinetics for the crystallization reaction.

More interesting is the thermal behaviour of the BGO(1:3) sample: XRD data indicated that crystallization, in fact, begins at 850 K with the formation of cubic $\text{Bi}_4\text{Ge}_3\text{O}_{12}$ only [18]. Starting from a molar ratio $\text{Bi}_2\text{O}_3:\text{GeO}_2 = 1:3$, we should have the separation of $\text{Bi}_2\text{Ge}_3\text{O}_9$ crystalline phase [19]; this was obtained by heat treatment of BGO(1:3) glassy sample at 1173 K for 48 h. Then the reaction can be written



followed by the step $\text{Bi}_4\text{Ge}_3\text{O}_{12} (\text{c}) + 3\text{GeO}_2 (\text{glass}) \rightarrow \text{Bi}_2\text{Ge}_3\text{O}_9 (\text{c})$. Because only crystalline phases separated in the temperature range investigated, the kinetics of the crystallization process for this sample was also analysed. Many approaches can be used to determine the kinetic parameters [20, 21] but we performed only isothermal measurements due to their greater accuracy.

Isothermal measurements were carried out by means of a PE computer program which allows scans at a fixed temperature and the calculation of the crystallized fraction as a function of time. Scans were performed at 843, 853, 863 and 873 K; the JMA equation [22] is usually used to describe the kinetics in a transformation reaction

$$x = 1 - \exp[-k(t - t_0)^n] \quad (5)$$

where x represents the fraction transformed after time t , t_0 is the incubation time, k is the rate constant and n is the reaction order parameter. In fact, t_0 is very small, so that we can assume $(t - t_0) \approx t$. k is considered to depend only on the temperature with an Arrhenius-like dependence

$$k = k_0 \exp(-\Delta E_a/RT) \quad (6)$$

where ΔE_a is the activation energy per mole, R is the gas constant and k_0 is a constant.

If we rewrite the Equation 5, according to the above assumption, in the form

$$\ln[-\ln(1-x)] = \ln k + n \ln t \quad (7)$$

we can plot $\ln[-\ln(1-x)]$ versus $\ln t$, obtaining a straight line with slope n and intercept $\ln k$. This computer program gives the partial areas of the reaction peaks, which are proportional to the volumetric fraction of crystallization, x . From these values, and using a least squares fit, four straight parallel lines were derived (Fig. 5) whose slope gives the reaction order parameters, n . In Table III the n values calculated from the crystallization curves are reported. The average value of n is equal to 1.10 ± 0.03 .

From Equation 6, it is also possible, by means of a least squares fit, to calculate the activation energy for the crystallization process of $\text{Bi}_4\text{Ge}_3\text{O}_{12}$ (Fig. 6); a value of $47.1 \pm 0.2 \text{ kcal mol}^{-1}$ is obtained.

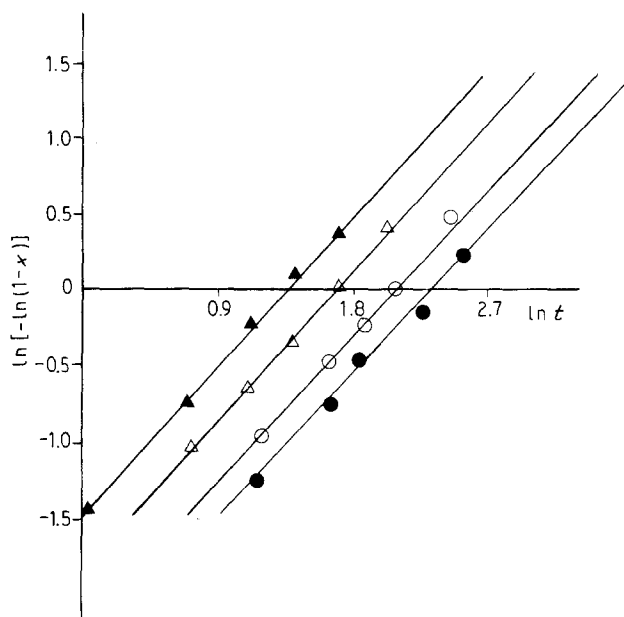


Figure 5 Least squares fits of $\ln[-\ln(1-x)]$ versus $\ln t$ for sample BGO(1:3) at different temperatures. Errors are smaller than the point size. (\blacktriangle) 873 K, (\triangle) 863 K, (\circ) 853 K, (\bullet) 843 K.

TABLE III. Kinetic data from isothermal measurements for BGO (1:3)

T (K)	n (± 0.03)	$\ln k$ (± 0.01)	R_2
843	1.07	-2.46	0.999
853	1.12	-2.29	0.997
863	1.11	-1.86	0.998
873	1.11	-1.47	0.998

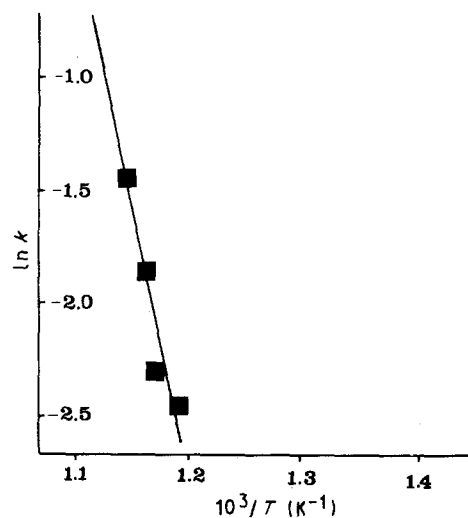


Figure 6 Least squares fits of $\ln k$ versus $10^3/T$ for sample BGO(1:3). Errors are smaller than the point size.

To obtain further information on the crystallization mechanism we also performed microphotographic analysis. Fig. 7 shows a scanning electron micrograph of BGO(1:3) after heating and leaching treatment: irregular pyramide-shaped microcrystals of $\text{Bi}_4\text{Ge}_3\text{O}_{12}$ can be seen rising up from the glassy matrix. This is consistent with a three-dimensional growth of particles. From the value of n calculated

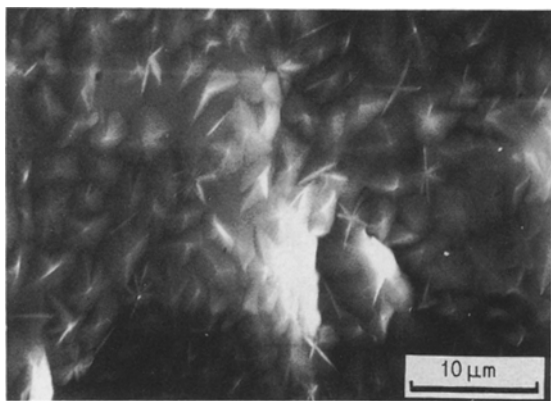


Figure 7 Scanning electron micrograph of sample BGO(1:3) treated at 840 K and leached.

(1.10 ± 0.03) it is possible to propose a diffusion-controlled crystallization mechanism, approximating n to the value of $n = 1.5$ valid for an instantaneous process (nucleation rate equal to zero) [22].

4. Conclusions

The optical and thermal behaviour of glassy BGO samples has been studied. Owing to instrumental limits, it is impossible to determine exactly the shape of the ultraviolet spectra, but we can suppose a charge-transfer absorption mechanism. The cut-off wavelengths have been measured. Thermal measurements allow confirmation that in the devitrification process the $\text{Bi}_2\text{O}_3:\text{GeO}_2$ ratio plays a fundamental role. The Bi_2GeO_5 phase, except for BGO(1:1), is thermodynamically unstable and gives rise to crystalline $\text{Bi}_4\text{Ge}_3\text{O}_{12}$ and glassy GeO_2 . The crystallization of $\text{Bi}_4\text{Ge}_3\text{O}_{12}$ occurs at lower temperature in BGO(1:3) than in BGO(2:3) and kinetic measurements indicate a very fast process. On the other hand, in BGO(6:1) the large amount of glassy phase still present after thermal treatment indicates a slow separation of crystalline $\text{Bi}_{12}\text{GeO}_{20}$.

The value of T_c obtained was lower than those reported in the literature and this could be advantageous for obtaining polycrystalline BGO samples more easily. However, further work is needed to determine their physical properties for technological applications.

Acknowledgements

The authors thank Mr G. Foroni, Istituto di Chimica Generale ed Inorganica, University of Parma, for his contribution in performing ICP analyses, and Professor G. P. Bernardini and Dr M. Corazza, Centro Interdipartimentale di Servizi di Microscopia Elettronica e Microanalisi, University of Firenze, for their help with SEM.

References

1. D. P. BORTFELD and H. MEIER, *J. Appl. Phys.* **43** (1972) 5110.
2. J. LINK and J. FONTANELLA, *ibid.* **51** (1980) 4352.
3. H. SCHWEPPE, *IEEE Trans. Sonics Ultras.* **SU-16** (1969) 219.
4. R. MONCORGE, B. JACQUIER and G. BOULON, *J. Lumines.* **14** (1976) 337.
5. E. LORENZ, in "Recent Progress in BGO Development for High-resolution Calorimetry", Report Max Planck Institut für Physik, Munich 1984.
6. A. HOROWITZ and G. KRAMER, *J. Crystal Growth* **79** (1986) 296.
7. R. NITSCHKE, *J. Appl. Phys.* **36** (1965) 2358.
8. J. LIEBERTZ, *J. Crystal Growth* **5** (1969) 150.
9. H. von PHILIPSBORN, *ibid.* **11** (1971) 348.
10. G. CORSMIT, M. A. van DRIEL, R. J. ELSENAAR, W. van de GUCHTE, A. M. HOOGENBOOM and J. C. SENS, *ibid.* **75** (1986) 551.
11. Powder Diffraction File, Alphabetical Index Inorganic Phases, (JCPDS, 1985).
12. J. WONG and C. A. ANGELL, in "Glass Structure by Spectroscopy" (Dekker, New York and Basel, 1976) pp. 150–2.
13. J. M. STEVELS, in "Proceedings of the 11th International Congress on Pure and Applied Chemistry", Vol. **5** (1953) p. 519.
14. R. REISFELD and L. BOEHM, *J. Non-Cryst. Solids* **16** (1974) 83.
15. K. YVON, W. JETISCHKO and E. PARTHE, *J. Appl. Crystallogr.* **10** (1977) 73.
16. B. AURIVILLIUS, C. G. LINDBLOM and P. STENSON, *Acta Chem. Scand.* **18** (1964) 1555.
17. W. J. P. van ENCKEVORT and F. SMET, *J. Crystal Growth* **82** (1987) 678.
18. E. I. SPERANSKAYA and A. A. ARSHAKUNI, *Russ. J. Inorg. Chem.* **9** (1964) 226.
19. B. C. GRABMAIER, S. HAUSSUHL and P. KLUFERS, *Z. Kristallogr.* **149** (1979) 261.
20. A. MAROTTA and A. BURI, *Thermochim. Acta* **25** (1978) 155.
21. S. BORDAS, M. GELI, M. T. CLAVAGUERA-MORA and N. CLAVAGUERA, *J. Non-Cryst. Solids* **57** (1983) 209.
22. C. H. BAMFORD and C. F. H. TIPPER (eds), in "Reactions in the Solid State", Comprehensive Chemical Kinetics, Vol. **22**, (Elsevier, Amsterdam, 1980) p. 71.

Received 2 February

and accepted 19 November 1990